
Exploiting Record Similarity for Practical Vertical Federated Learning

Zhaomin Wu, Qinbin Li, Bingsheng He
National University of Singapore
{zhaomin,qinbin,hebs}@comp.nus.edu.sg

Abstract

As the privacy of machine learning has drawn increasing attention, federated learning is introduced to enable collaborative learning without revealing raw data. Notably, *vertical federated learning* (VFL), where parties share the same set of samples but only hold partial features, has a wide range of real-world applications. However, existing studies in VFL rarely study the “record linkage” process. They either design algorithms assuming the data from different parties have been linked or use simple linkage methods like exact-linkage or top1-linkage. These approaches are unsuitable for many applications, such as the GPS location and noisy titles requiring fuzzy matching. In this paper, we design a novel similarity-based VFL framework, FedSim, which is suitable for more real-world applications and achieves higher performance on traditional VFL tasks. Moreover, we theoretically analyze the privacy risk caused by sharing similarities. Our experiments on three synthetic datasets and five real-world datasets with various similarity metrics show that FedSim consistently outperforms other state-of-the-art baselines.

1 Introduction

The deployment of machine learning depends on the availability of data. As high-quality data are usually collected and held by multiple parties in practice, the collaboration among those parties can significantly boost the performance of certain machine learning tasks. However, due to privacy concerns and policy regulations, such collaborative learning has to be achieved without directly sharing raw data across parties. Under these circumstances, *federated learning* is proposed to enable collaborative training on distributed datasets without sharing raw data.

One important scenario of federated learning is *vertical federated learning* (VFL), where multiple parties share the same set of samples but have different sets of features. We focus on the setting where only one party holds the labels like most of the studies [8, 27, 34, 62]. In VFL, some features that exist on multiple parties are called *common features* (e.g., name, ID). The value (or vector) of common features in a data record is called its *identifier*. This scenario commonly exists in the real world and has been widely studied [33, 62, 66]. For example, a digital bank can collaborate with a FinTech company to estimate the credit scores of credit card applicants. In this example, the applicants’ name and address are common features.

There two main processes in VFL: linkage and training. In the linkage process, the datasets on different parties are linked according to the identifiers. Specifically, the data records with the same or similar identifiers are linked as a sample. Then, in the training process, these distributed but linked samples are trained by VFL algorithms. As studied in [40], besides the training process, the linkage process can also significantly affect the performance of VFL models.

Most of the existing VFL approaches [9, 16, 25, 35, 57, 70] focus on the training process and simply assume that linkage process has already been done. This strong assumption hinders these

approaches from real-world applications. Some other approaches [9, 34, 36, 37, 49, 62] adopt *private set intersection* (PSI) [7] to link the data records that share exactly the same identifier. Nonetheless, in many real-world cases, either the identifier cannot be linked exactly (e.g., GPS location) or some true matches can be neglected by exact linkage [46] (e.g., address). Hence, these approaches suffer performance loss and can only handle limited real-world scenarios.

To solve the limitations of exact linkage, by adopting *privacy preserving record linkage* (PPRL) [56], some approaches [21, 27, 40] calculate the similarities between identifiers and only link data records with the highest similarities. In [27], the authors follow the linkage process of [40] and apply semi-supervised learning techniques to estimate missing values of unlinked data records. However, as shown in our experiments, only linking the most similar data records can cause significant performance loss especially on datasets with fuzzy identifiers (e.g., GPS locations). Moreover, [27, 40] assume that there exists a one-to-one mapping between the data records across parties, which is impractical in many applications.

Simply upgrading the PPRL method cannot fully eliminate the performance loss of VFL caused by the linkage. Because the original goal of PPRL is to accurately link all *true-matched pairs* [56], while the linkage process before VFL aims to keep all *beneficial pairs* that may contribute to the training process regardless of whether they are true-matched or not. The number and significance of beneficial pairs vary considerably in different datasets and even in different samples. Taking housing price prediction as an example. As shown in Figure 1, for some remote records (e.g. villages), only a few close records might be beneficial. But for some records in large clusters (e.g., cities), they can benefit from many records around.

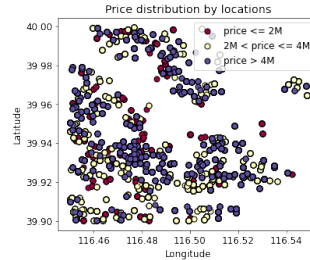


Figure 1: Housing price distribution by locations in Beijing

Though it is hard to find all beneficial pairs, finding a superset of beneficial pairs (i.e., possible beneficial pairs) is much easier by keeping top- K similar identifiers, where K is large enough. The main challenge is how to effectively exploit these possible beneficial pairs and their similarities to boost the performance of VFL.

To tackle this challenge, we propose a similarity-based VFL framework FedSim on the top of SplitNN [57], which is a VFL algorithm¹ for neural networks. By considering possible beneficial pairs and similarities in the training process, FedSim not only can be applied to a wider range of scenarios that traditional VFL cannot handle but also provides close or better performance on the traditional tasks of VFL. Our main contributions include: 1) an effective similarity-based VFL framework (FedSim); 2) theoretical analysis on the privacy of FedSim; 3) collecting five real-world datasets for vertical federated learning; 4) extensive experiments on three synthetic datasets and five real-world datasets, which show that FedSim consistently outperforms state-of-the-art baselines.

2 Background

Privacy-Preserving Record Linkage *Privacy-preserving record linkage* (PPRL) aims to link the data records from multiple parties that refer to the same sample without revealing real identifiers. Most of the PPRL methods [17, 28, 30, 31, 55] consist of three main steps: blocking, comparison and classification. First, in the blocking step, data records that are unlikely to be linked are pruned to reduce the number of comparisons. Then, in the comparison step, a similarity between identifiers is computed for each candidate pair of data records. Finally, in classification, each candidate pair is classified as “matches” or “non-matches”, which is usually done by a manually set threshold.

The similarities in the comparison step are calculated based on negative distances between identifiers. Different distance metrics are applied according to the type of identifiers and PPRL framework. For numeric identifiers, some approaches [26, 32] calculate similarities based on Euclidean distances. Some approaches [30, 54] convert the numeric values to anonymous bloom filters and calculate similarities based on Hamming distances between bloom filters. For string identifiers, some approaches [29, 48] calculate similarities by Levenshtein distances between strings. Some approaches [10, 28, 30, 59] convert the strings to bloom filters and calculate similarities based on Hamming distances. FedSim does not rely on specific similarity metrics while the quality of similarities may affect

¹SplitNN is classified as split learning in some studies. For simplicity, we denote SplitNN as a VFL algorithm.

the performance. We adopt a state-of-the-art PPRL framework FEDERAL [30] to generate bloom filters in our analysis and experiments for Hamming-based similarities, which is briefly introduced in Appendix B.

SplitNN The main idea of SplitNN is to split a model into multiple parties and conduct training by transferring gradients and intermediate outputs across parties. As shown in Figure 2, a global model is split into θ^{A1} , θ^{A2} , and θ^B . In each iteration, the output of model θ^B is calculated by forward-propagation and sent to party A which holds the labels. Party A concatenates the outputs of local models θ^{A1} and θ^B , and continues forward propagation to predict \hat{y} . Then, party A calculates loss between \hat{y} and real labels and performs back-propagation until the input of aggregation model θ^{A2} . The gradients w.r.t. the outputs of θ^B are sent to party B. Finally, both parties finish backward propagation with corresponding gradients.

The privacy of the transferred intermediate results can be protected by NoPeek [58]. NoPeek can prevent SplitNN from reconstruction attacks where attackers attempt to reconstruct raw data from intermediate representations.

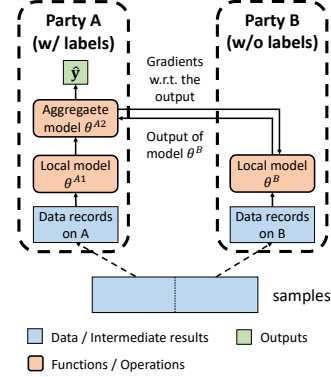


Figure 2: Structure of SplitNN

3 Related Work

Most studies (e.g., [24, 25, 39, 47, 57, 70]) in VFL focus on training and simply assumes record linkage has been done (i.e., implicit exact linkage on record ID), which is impractical since most real-world federated datasets are unlinked. Some approaches exactly link the identifiers by exact PPRL [9] or private set intersection (PSI) [9, 36, 37, 49, 62]. However, these approaches incur performance loss of VFL and are also impractical since the common features of many real-world federated datasets cannot be exactly linked (e.g. GPS location). In [21], the authors greedily link the most similar identifiers in PPRL, which negatively impacts performance since some beneficial pairs with relatively low similarity may be neglected. In [40] (also adopted by [27]), the authors explore the impact of record linkage on the performance of VFL. However, they also focus only on the most similar identifiers and assume there is a one-to-one mapping between the data records of two parties, which is not always true in practice.

Table 1: Summary of existing VFL algorithms and their adopted PPRL methods

Category	Research Work	Training & Linkage Method
Top1Sim	[21, 27, 40]	Comparison + Top1-classification + VFL
Exact	[9, 34, 36, 37, 44, 49, 62, 64]	Comparison + Exact-classification + VFL
Exact (Implicit)	[6, 8, 16, 19, 20, 24, 25, 35, 39, 47, 52, 57, 60, 61, 65, 67, 69, 70]	[Comparison + Exact-classification] + VFL
FedSim	Our proposal	Comparison + VFL

Current VFL frameworks support various machine learning models including linear regression [16], logistic regression [24], support vector machine [35], gradient boosting decision trees [9, 62]. FDML [25] supports neural networks but it requires all the parties to hold labels. SplitNN [57] focuses on neural networks and provides a new idea of collaborative learning where the model is split and held by multiple parties. Since we study the scenario where only one party holds the labels and want to support commonly used neural networks, we build FedSim on top of SplitNN.

4 Our Approach: FedSim

4.1 Problem Formulation

Suppose there are two parties A, B which want to coordinate with each other to train a machine learning model. Party A holds m samples and their corresponding labels $\{x_i^A, y_i\}_{i=1}^m$. Party B holds n samples $\{x_i^B\}_{i=1}^n$ which can also benefit the machine learning task. Besides, there is an honest-but-curious third party, party C, which coordinates the PPRL process. In order to perform

linkage, we assume there are some common features between the $\{x_i^A\}_{i=1}^m$ and $\{x_i^B\}_{i=1}^n$, i.e., $\{x_i^A\}_{i=1}^m = \{d_i^A, k_i^A\}_{i=1}^m$, $\{x_i^B\}_{i=1}^n = \{d_i^B, k_i^B\}_{i=1}^n$, where k_i^A, k_i^B are common features used for linkage and d_i^A, d_i^B are remaining features used for training with dimension l_A, l_B . The type of common features is determined by the dataset and PPRL method, which can be numeric values, strings, or bloom filters. We also assume the distances $\text{dist}(k_i^A, k_j^B)$ between possible beneficial pairs, denoted as \mathbf{D} , have been calculated by PPRL and stored in Party C, which is a necessary step of most PPRL frameworks [17, 30, 32, 53]. Our goal is to enable party A to exploit \mathbf{x}^B and \mathbf{D} to train a model that minimizes the global loss. Formally, denoting $\mathbf{x}^A \triangleq \{x_i^A\}_{i=1}^m$, $\mathbf{x}^B \triangleq \{x_i^B\}_{i=1}^n$, $\mathbf{y} \triangleq \{y_i\}_{i=1}^m$, $\mathbf{d}^A \triangleq \{d_i^A\}_{i=1}^m$, $\mathbf{d}^B \triangleq \{d_i^B\}_{i=1}^n$, we aim to optimize the following formula.

$$\min_{\theta} \frac{1}{m} \sum_{i=1}^m L(f(\theta; x_i^A, \mathbf{x}^B, \mathbf{D}); y_i) + \lambda \Omega(\theta)$$

where $L(\cdot)$ is the loss function, $f(\cdot)$ is the VFL model, and $\lambda \Omega(\theta)$ is the regularization term.

Threat Model We assume parties A, B, and C are honest-but-curious (HBC) and do not collude with each other. Party A holds data matrix $\mathbf{x}^A = [\mathbf{d}^A, \mathbf{k}^A]$ and similarities \mathbf{s} . Party B holds data matrix $\mathbf{x}^B = [\mathbf{d}^B, \mathbf{k}^B]$. Party C holds some intermediate results during the calculation of distances \mathbf{D} , which is determined by the PPRL method. An attacker can be one of the parties or an outsider who wants to infer the unknown information mentioned above.

4.2 Overview

Our approach has two components: fuzzy linkage and similarity-based VFL. In fuzzy linkage, after finding possible beneficial pairs by existing PPRL methods, party C preprocesses the similarities by normalization and perturbation with Gaussian noise. The scale of noise can be determined by a constant bound τ of the attacker’s success rate, which is further analyzed in Section 5. Then, the aligning information and aligned similarities are sent to party A or B which will align the data records accordingly. In similarity-based VFL, we design a model (as shown in Figure 5) by adding additional components around SplitNN to effectively exploit similarities. Finally, this model, taking the aligned data records and aligned similarities as input, is trained by back-propagation like SplitNN.

4.3 Fuzzy linkage

The process of fuzzy linkage is summarized in Figure 3. In step 1, each sample in A, together with K samples with the smallest distances in B, are selected as possible beneficial pairs. The distances between possible beneficial pairs are calculated by a PPRL protocol. To fully utilize \mathbf{x}^B for each sample x_i^A , K should be large enough to ensure all beneficial pairs are included. In step 2, party C calculates the similarities as normalized negative distances. Formally, the raw similarity ρ_{ij} between x_i^A and x_j^B is defined as

$$\rho_{ij} = \frac{-\text{dist}(k_i^A, k_j^B) - \mu_0}{\sigma_0} \quad (1)$$

where μ_0 and σ_0 are the mean and standard variance of all negative distances $-\text{dist}(k_i^A, k_j^B)$. To prevent the attacker from guessing the vectors k_i^A or k_j^B from similarities (further discussed in Section 5), we add Gaussian noise of scale σ to each ρ_{ij} . Formally, for $\forall i \in [1, m], \forall j \in [1, K]$

$$s_{ij} = \rho_{ij} + N(0, \sigma^2) \quad (2)$$

For simplicity, we denote $\mathbf{s}_i \triangleq \{s_{ij}\}_{j=0}^K$ and $\mathbf{s} \triangleq \{\mathbf{s}_i\}_{i=0}^m$.

After the similarities are calculated, party C directly sends the similarities \mathbf{s} to party A and sends the aligning information to both parties. In step 3, party A and B align their samples or similarities according to the aligning information to ensure that each x_i^A , \mathbf{x}_i^B and \mathbf{s}_i refer to the same sample.

4.4 Similarity-Based Vertical Federated Learning

The training process is summarized in Algorithm 1 and the model structure of FedSim is shown in Figure 5. As discussed in Section 3, FedSim is designed on top of SplitNN [57], which makes preliminary predictions \mathbf{o}_i (with l_m dimensions) for each d_i^A and its K neighbors \mathbf{d}_i^B (lines 4-9).

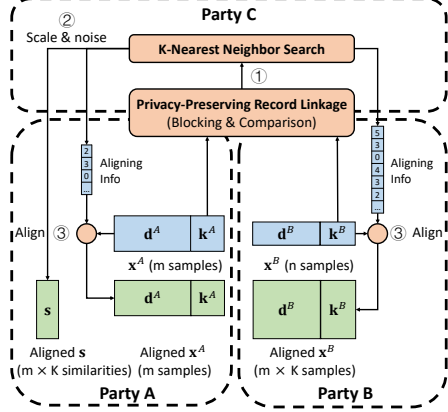


Figure 3: Procedure of fuzzy linkage

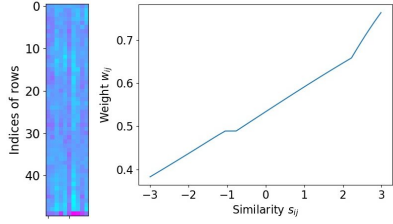


Figure 4: Visualization of converged models

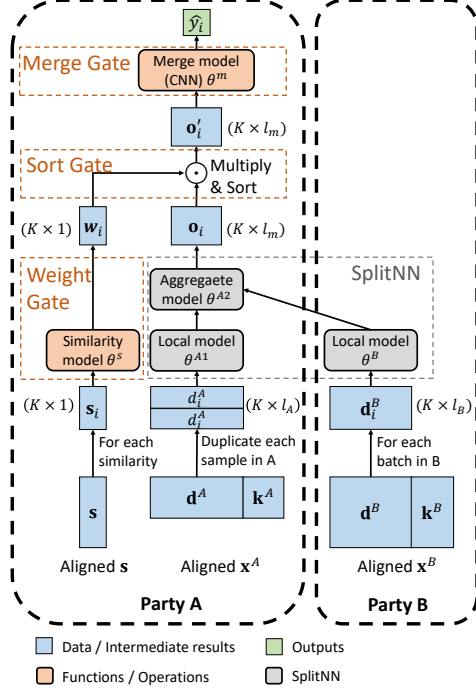


Figure 5: Model structure of FedSim

Specifically, we add three *gates* (weight gate, merge gate, sort gate) around SplitNN and train the whole model by back-propagation like SplitNN. The main function of the three gates is to effectively exploit similarities s_i to merge the preliminary outputs o_i into the final prediction \hat{y}_i . For simplicity, we use $\theta_i^A = \{\theta_i^{A1}, \theta_i^{A2}\}$ to denote all the SplitNN parameters in party A at iteration t .

Weight Gate One straightforward idea is that more similar pairs of samples contribute more to the performance. Thus, the rows in o_i with higher similarities should be granted a larger weight. Directly multiplying the similarities to o_i is inappropriate since the values of similarities do not represent the actual contribution. Therefore, in weight gate, we use *similarity model*, a simple neural network with one-dimensional input and one-dimensional output, to map the similarities to weights w_i which indicates the contribution to the final loss (line 10). Then, the weighted outputs are calculated as a matrix multiplication (line 11).

Merge Gate The merge gate contains a merge model to aggregate the information in o'_i (line 13). For tasks that only require a linear aggregation, setting merge model as an average over rows of o'_i is sufficient to obtain a promising result. However, for tasks that require a non-linear aggregation, a neural network is required to be deployed as a merge model. In this case, although merge model can be implemented by a multi-layer perceptron (MLP) which takes flattened o'_i as input, such an approach usually leads to over-fitting due to a large number of parameters. Meanwhile, the flatten operation causes information loss because merge model is unaware of which K features in the flattened o'_i correspond to the same output feature in o'_i . Considering these two factors, we implement merge model with 2D convolutional neural networks (CNN) with kernel size $k_{conv} \times 1$, which effectively merge the samples with close similarities with much fewer parameters than that in MLP.

Sort Gate The sort gate is an auxiliary module for merge gate and is optional depending on the property of the chosen merge model. For merge models that are insensitive to the order of o'_i (e.g., averaging over rows), sorting is not needed because the order does not affect the output of merge model. However, for merge models that are sensitive to the order of o'_i (e.g., neural networks), inconsistent order of features can incur irregular sharp gradients which makes merge model hard to converge. Therefore, it is necessary to sort o'_i by similarities (line 12) to stabilize the updates on merge model. Meanwhile, grouping the pairs with close similarities together helps merge gate effectively aggregate the information.

Algorithm 1: Training Process of FedSim

Input : Aligned datasets and labels $\mathbf{d}^A, \mathbf{d}^B, \mathbf{y}$; similarities \mathbf{s} ; number of similar samples K ; number of epochs T ; number of samples m in party A;
Output : SplitNN parameter θ_t^A, θ_t^B ; similarity model parameter θ_t^s ; merge model parameter θ_t^m

```
1 Initialize  $\theta_0^A, \theta_0^B, \theta_0^s, \theta_0^m$ 
2 for  $t \leftarrow 0$  to  $T$  do
3   for  $i \leftarrow 0$  to  $m$  do
4     Party B
5     loads  $i$ -th batch  $\mathbf{d}_i^B$  from  $\mathbf{d}^B$ 
6     calculates  $\mathbf{c}_i = f(\theta_t^B; \mathbf{d}_i^B)$  and sends the  $\mathbf{c}_i$  to party A
7     Party A
8     loads  $i$ -th sample  $d_i^A$  from  $\mathbf{d}^A$ 
9     receives  $\mathbf{c}_i$  from party B and calculates the output matrix  $\mathbf{o}_i = f(\theta_t^A; \mathbf{c}_i, d_i^A)$ 
10    loads similarities  $\mathbf{s}_i$  from  $\mathbf{s}$  and calculates weights  $\mathbf{w}_i = f(\theta_t^s; \mathbf{s}_i)$ 
11    calculates weighted outputs  $\mathbf{o}'_i = \text{diag}(\mathbf{w}_i)\mathbf{o}_i$ 
12    sorts the rows of  $\mathbf{o}'_i$  by  $\mathbf{s}_i$  (or  $\mathbf{w}_i$ )
13    feeds the sorted  $\mathbf{o}'_i$  to merge model and calculates the final output  $\hat{y}_i = f(\theta_t^m; \mathbf{o}'_i)$ 
14    calculates gradients  $\mathbf{g}_t^A = \nabla_{\theta_t^A} L(\hat{y}_i, y_i)$ ,  $\mathbf{g}_t^s = \nabla_{\theta_t^s} L(\hat{y}_i, y_i)$ ,  $\mathbf{g}_t^m = \nabla_{\theta_t^m} L(\hat{y}_i, y_i)$ ,
     $\mathbf{g}_t^c = \nabla_{\mathbf{c}_i} L(\hat{y}_i, y_i)$  and sends  $\mathbf{g}_t^c$  to party B
15    Party B receives  $\mathbf{g}_t^c$  from party A and continues calculating gradients  $\mathbf{g}_t^B = \nabla_{\theta_t^B} \mathbf{g}_t^c$ 
16    Party A & B respectively updates their parameters
     $\theta_{t+1}^A = \theta_t^A - \eta_t \mathbf{g}_t^A, \theta_{t+1}^B = \theta_t^B - \eta_t \mathbf{g}_t^B, \theta_{t+1}^s = \theta_t^s - \eta_t \mathbf{g}_t^s, \theta_{t+1}^m = \theta_t^m - \eta_t \mathbf{g}_t^m$ 
```

The whole model with SplitNN and three gates is trained with back-propagation by transferring gradients like SplitNN (lines 14-15). After gradients are calculated, all the parameters are updated synchronously in each round (line 16).

To provide more insights of FedSim, we visualize the similarity model and the merge model as Figure 4, both of which are extracted from the converged FedSim on game dataset (see Section 6). For merge model (left), we evaluate the feature importance of each feature in \mathbf{o}'_i (100×10) by integrated gradients [50], which is widely used [41, 45] in model explanation. The warmer color indicates higher importance and the colder color indicates lower importance. Since rows with larger similarities are granted higher indices after the sorting, it can be observed that the features with larger similarities are more important than the features with a lower index. For similarity model (right), which has one-dimensional input and one-dimensional output, we plot the model in a two-dimensional coordinate system when scaled similarities range in $[-3, 3]$. It can be found that the rows with higher similarities have higher weights, thus more influence on the final output. Both merge model and similarity model cooperate to filter through informative features and generate accurate predictions. These observations well match the principles of our designs.

5 Privacy of FedSim

5.1 Overall Analysis

The shared information during the training and linkage process includes: 1) similarities \mathbf{s} that are shared to Party A; 2) intermediate results $\{\mathbf{c}_i\}_{i=1}^m$ in SplitNN that are shared to Party A; 3) intermediate results in PPRL that are shared to Party C.

The intermediate results in SplitNN and PPRL are respectively studied in [58] and [30] (see Section 2 for details), both of which are orthogonal to this paper. Therefore, we study the privacy risk caused by similarities \mathbf{s} . According to Equation 1 and 2, each similarity s_{ij} is calculated from k_i^A and k_j^B . Therefore, party A, as a potential attacker, may try to reversely predict k_j^B from some identifiers $\{k_i^A | i \in S\}$ and the corresponding similarities $\{s_{ij} | i \in S\}$, where S is the set of indices of used identifiers.

As discussed in Section 2, our privacy analysis is based on the assumption that \mathbf{k}^A and \mathbf{k}^B are bloom filters, the distances of which are integers. Our analysis focuses on a greedy attacker who first predicts the most likely distance from each s_{ij} and then predicts the most likely bloom filter from the predicted distance. Assuming the attacker already knows the scaling parameters μ_0, σ_0 , we formulate the attacker method as follows.

Attack Method To obtain \hat{k}_j^B as a prediction of k_j^B , the attacker 1) predicts a set of raw similarities $\hat{\rho}_{ij}$ ($i \in S$) from s_{ij} ($i \in S$), respectively, by maximum a posteriori (MAP) estimation with Gaussian prior $N(\mu_0, \sigma_0)$, i.e., $\hat{\rho}_{ij} = \arg \max_{\rho_{ij}} p(\rho_{ij} | s_{ij})$; 2) calculates each distance \hat{u}_{ij} by scaling back $\hat{\rho}_{ij}$ with parameters μ_0, σ_0 , i.e., $\hat{u}_{ij} = -\sigma_0 \hat{\rho}_{ij} - \mu_0$ ($i \in S$); 3) uniformly guesses \hat{k}_j^B from all possible values satisfying $\forall i \in S, \text{dist}(k_i^A, \hat{k}_j^B) = \hat{u}_{ij}$, because these possible values have the same probability of being the real k_j^B .

Besides the greedy attack, advanced attackers may predict through the probability distribution of distances rather than predict through the most likely distance. Some attackers may even know some side information like the prior distribution of k_j^B and employ this side information to launch attacks. We do not cover these advanced attacks in this paper and will leave them as our future work.

5.2 Privacy Guarantee

Although disclosing a bloom filter to the attacker is not catastrophic since it is infeasible to reversely infer the raw features from the bloom filters, which is proved in [30], we aim to bound the probability of such disclosure by a small amount. If an attacker follows the attack model, we find that no matter how the attacker selects the set S , the probability of predicting the correct k^B is always bounded by a small constant related to σ_0 and σ . The proof of Theorem 1 is included in Appendix A.

Theorem 1. *Given a finite set of perturbed similarities s_{ij} ($i \in S$) between $|S|$ bloom-filters b_i^A ($i \in S$) in party A and one bloom filter k_j^B in party B, if an attacker knows the scaling parameters μ_0, σ_0 and follows the procedure of the attack method, the probability of the attacker’s predicted bloom filter \hat{k}_j^B equaling the real bloom filter k_j^B is bounded by a constant τ . Formally,*

$$\Pr \left[\hat{k}_j^B = k_j^B \mid \{s_{ij} | i \in S\}, \{k_i^A | i \in S\}, \mu_0, \sigma_0 \right] \leq \tau = \text{erf} \left(\frac{\sqrt{\sigma^2 + 1}}{2\sqrt{2}\sigma\sigma_0} \right)$$

where $\text{erf}(\cdot)$ is error function, i.e., $\text{erf}(x) = \frac{2}{\sqrt{\pi}} \int_0^x e^{-t^2} dt$.

From Theorem 1, we conclude that there are two factors that affect the attacker’s success rate: 1) noise added to the similarity (σ); 2) standard variance of bloom filters (σ_0). Among these factors, σ_0 determines the lower bound of the success rate because $\sqrt{\sigma^2 + 1}/(2\sqrt{2}\sigma\sigma_0) < 1/(2\sqrt{2}\sigma_0)$. σ determines how close success rates FedSim can guarantee compared to the lower bound. When σ is large enough, increasing σ helps little with reducing the success rate. Therefore, to ensure the good privacy of FedSim, we should first guarantee a large enough variance among the bloom filters and then add a moderate noise to the similarities.

Taking *house* dataset (see Section 6.1) as an example where $\sigma_0 = 21178.86$. By setting $\sigma = 0.4$, we have $\tau = 0.0051\%$. Considering the 19479 samples in the training set of party B, the expected number of disclosed bloom filters is 0.988, indicating less than a single bloom filter is expected to be disclosed.

6 Experiment

6.1 Experiment Setup

Dataset We evaluate FedSim on three synthetic datasets (`sklearn` [11], `frog` [14], `boone` [15]) and five real-world datasets (`house` [1, 42], `taxi` [3, 51], `hdb` [23, 63], `game` [12, 22], `song` [2, 13]). The detailed information of datasets are summarized in Appendix C. For each real-world dataset, we collect two public datasets from different real-world parties and conduct VFL on both public datasets. For each synthetic dataset, we first create a global dataset by generating with `sklearn` API [11] (`sklearn`) or collecting from public (`frog`, `boone`). Then, we randomly select some features as common features and randomly divide the remaining features equally to both parties. For a fair comparison, common features are not used in training in all experiments. To simulate the real-world

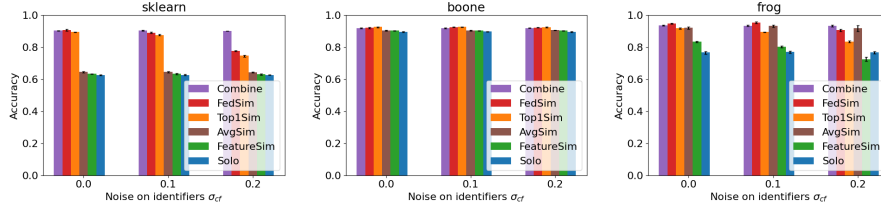


Figure 6: Performance on synthetic datasets with Euclidean-based similarity

applications, we also add different scales σ_{cf} of Gaussian noise to the common features. Specifically, for each identifier \mathbf{v}_i , the perturbed identifier $\mathbf{v}'_i = \mathbf{v}_i + N(\sigma_{cf}^2 \mathbf{I})$ will be used for linkage.

Baselines We compare FedSim with six baselines in our experiments: 1) Solo: Only the dataset in party A (\mathbf{d}^A) is trained; 2) Combine: The global dataset ($[\mathbf{d}^A, \mathbf{d}^B]$) is trained by MLP (only applicable for synthetic datasets); 3) Exact (adopted by [9, 34, 36, 37, 44, 49, 62, 64]): Only the samples with exactly the same identifiers are linked and fed into SplitNN; 4) Top1Sim (adopted by [21, 27, 40]): Each sample in party A is linked with the most similar sample in party B and fed into SplitNN; 5) AvgSim: For each sample in party A and its K most similar samples, the K outputs of SplitNN are averaged as the prediction of this sample; 6) FeatureSim: For each sample in party A and its K most similar samples, the similarity is appended as a feature. Among these baselines, Top1Sim, AvgSim, FeatureSim require similarity-based PPR. For fair comparison, we ensure the three baselines and FedSim are trained based on the same K , the same linkage result, and the same similarities. Exact is only evaluated on game and song because no exactly matched identifiers can be found on other datasets.

Training Similarity model is a multi-layer perception (MLP) with one hidden layer. Merge model contains a 2D convolutional layer with kernel ($k_{conv} \times 1$) followed by a dropout layer and an MLP with one hidden layer. Both the local model and aggregate model in SplitNN are MLPs with one hidden layer. We adopt LAMB [68], the state-of-the-art large-batch optimizer, to train all the models. The number of neighbors K is chosen from $\{50, 100\}$. Each dataset is split into training, validation, and test set with ratios 0.7, 0.1, 0.2. We run each algorithm five times and report the mean and standard variance (range is reported instead in figures) of performance on the test set. We present root mean square error (RMSE) and R-squared value (R^2) for regression tasks and present accuracy for classification tasks. The choice of other hyperparameters is presented in Appendix C.

In Section 6.2, we evaluate the performance of FedSim on different similarity metrics. In Section 6.3, we evaluate how our privacy mechanisms affect the performance of FedSim. In Appendix D, we compare the training time between FedSim and baselines. In Appendix E, we present how the choice of K affects the performance.

6.2 Performance

Table 2: Performance on real-world datasets with Euclidean-based similarity

Algorithms	house		bike		hdb	
	RMSE	R^2	RMSE	R^2	RMSE	R^2
Solo	75.37±0.36	0.8311±0.0016	273.86±0.75	0.5965±0.0022	29.89±0.16	0.9631±0.0004
Exact	-	-	-	-	-	-
Featuresim	66.46±0.37	0.8687±0.0015	275.51±0.88	0.5916±0.0026	37.34±0.25	0.9424±0.0008
AvgSim	51.85±0.48	0.9201±0.0015	239.61±0.08	0.6911±0.0002	53.09±0.15	0.9162±0.0005
Top1sim	58.52±0.31	0.8982±0.0011	256.63±0.88	0.6457±0.0025	31.25±0.12	0.9597±0.0003
FedSim	43.02±0.19	0.9450±0.0005	237.04±0.44	0.6977±0.0011	27.28±0.12	0.9693±0.0003

Euclidean-Based Similarity To evaluate FedSim on Euclidean-based similarities, we conduct experiments on three synthetic datasets (Figure 6) and three real-world datasets (Table 2) with numeric identifiers. From the results, we can make three observations. First, FedSim has better or close performance compared to all the baselines. For example, in house, FedSim reduces RMSE by 27% compared to Top1Sim and by 17% compared to AvgSim. Second, FedSim is less affected by the noise on the identifiers compared to Top1Sim. For example, in frog, the accuracy of Top1Sim

drops to around 84% as the noise scale reaches 0.2, while the accuracy of FedSim remains around 91%. Third, in synthetic datasets with small scale σ_{cf} of noise, FedSim even slightly outperforms Combine, which was expected to be an upper bound. That indicates that even when there exists an exact one-to-one mapping, directly performing exact linkage does not always lead to the best performance, which is because the information in common features is neglected in Combine.

Levenshtein-Based Similarity To evaluate FedSim on Levenshtein-based similarities, we conduct experiments on two real-world datasets with string identifiers (Table 3). From Table 3, we observe that FedSim still outperforms all the baseline but the improvement is less significant compared to the datasets with numeric identifiers (Table 2). That is because in game and song, the pairs whose titles are different are less likely to contribute to VFL, thus in both cases, Exact and Top1Sim can achieve a relatively good performance.

Table 3: Performance on real-world datasets with Levenshtein-based similarity

Algorithms	game	song	
	Accuracy	RMSE	R^2
Solo	81.67±0.27%	8.06±0.02	0.3409±0.0027
Exact	92.71±0.06%	8.07±0.01	0.3403±0.0008
Featuresim	90.97±0.18%	8.00±0.02	0.3504±0.0025
Avgsim	90.68±0.10%	8.01±0.02	0.3495±0.0034
Top1sim	92.57±0.19%	8.14±0.01	0.3278±0.0009
FedSim	92.93±0.17%	8.00±0.01	0.3508±0.0022

Hamming-Based Similarity The performance of FedSim on Hamming-based similarities is presented in Section 6.3, where we further study how noise on similarities affects the performance.

6.3 Privacy

In this subsection, to study how additional noise on similarities affects the performance of FedSim, we conduct experiments on five real-world datasets. We convert the string or numeric identifiers to bloom filters according to [30] and insert Gaussian noise with scale σ to the similarities according to Section 4.3. Each σ is calculated from a bound τ according to Theorem 1. The results are presented in Figure 7. Exact is not evaluated here because few bloom filters have exactly the same bits.

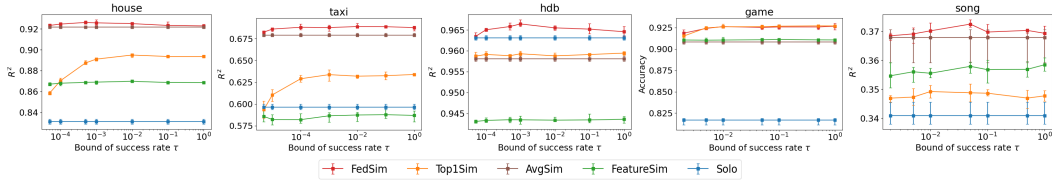


Figure 7: Performance of FedSim on real-world datasets with Hamming-based similarity

From Figure 7, we can make two observations. First, surprisingly, FedSim achieves the best performance at a moderate level of noise on most datasets. This is consistent with many studies [4, 5, 18, 43] that show injecting a small scale of noise on the input can reduce overfitting and improve the performance of neural networks. More specifically, according to [4], white noise on the input is equivalent to ℓ_2 -regularization in certain cases. Therefore, such noise addition can be regarded as a regularization method which only has effect on similarities. Second, as the scale of noise and dataset varies, the performance of Top1Sim and AvgSim is very unstable. For example, Top1Sim has close performance to FedSim on game with small scale of noise (large τ), but has poor performance on house and hdb. AvgSim has good performance on house but poor performance on hdb and game. Nevertheless, FedSim remains relatively persistent performance with varying τ and is always better than or close to all the baselines.

7 Conclusion

In this paper, we propose FedSim, a novel VFL framework based on similarities to overcome the drawback of the existing VFL approaches. FedSim boosts the performance of VFL by directly utilizing the similarities calculated in PPRL and skipping the classification process. We also theoretically analyze the additional privacy risk introduced by sharing similarities and provide a bound for the attacker’s success rate. In our experiment, FedSim consistently outperforms other baselines.

References

- [1] Airbnb. Airbnb prices in Beijing. <http://insideairbnb.com/get-the-data.html>.
- [2] Thierry Bertin-Mahieux, Daniel PW Ellis, Brian Whitman, and Paul Lamere. The million song dataset. 2011.
- [3] Citi Bike. Citi bike system data. <https://www.citibikenyc.com/system-data>.
- [4] Chris M Bishop. Training with noise is equivalent to tikhonov regularization. *Neural computation*, 7(1):108–116, 1995.
- [5] Christopher M Bishop et al. *Neural networks for pattern recognition*. Oxford university press, 1995.
- [6] Iker Ceballos, Vivek Sharma, Eduardo Mugica, Abhishek Singh, Alberto Roman, Praneeth Vepakomma, and Ramesh Raskar. Splitnn-driven vertical partitioning. *arXiv preprint arXiv:2008.04137*, 2020.
- [7] Hao Chen, Kim Laine, and Peter Rindal. Fast private set intersection from homomorphic encryption. In *Proceedings of the 2017 ACM SIGSAC Conference on Computer and Communications Security*, pages 1243–1255, 2017.
- [8] Tianyi Chen, Xiao Jin, Yuejiao Sun, and Wotao Yin. Vaf1: a method of vertical asynchronous federated learning. *arXiv preprint arXiv:2007.06081*, 2020.
- [9] Kewei Cheng, Tao Fan, Yilun Jin, Yang Liu, Tianjian Chen, and Qiang Yang. Secureboost: A lossless federated learning framework. *arXiv preprint arXiv:1901.08755*, 2019.
- [10] Peter Christen, Thilina Ranbaduge, Dinusha Vatsalan, and Rainer Schnell. Precise and fast cryptanalysis for bloom filter based privacy-preserving record linkage. *IEEE Transactions on Knowledge and Data Engineering*, 31(11):2164–2177, 2018.
- [11] David Cournapeau. Sklearn API. https://scikit-learn.org/stable/modules/generated/sklearn.datasets.make_classification.html#sklearn.datasets.make_classification.
- [12] Nik Davis. Steam store games (clean dataset). <https://www.kaggle.com/nikdavis/steam-store-games>.
- [13] Michaël Defferrard, Kirell Benzi, Pierre Vandergheynst, and Xavier Bresson. Fma: A dataset for music analysis. *arXiv preprint arXiv:1612.01840*, 2016.
- [14] Dheeru Dua and Casey Graff. UCI machine learning repository, 2017.
- [15] Dheeru Dua and Casey Graff. UCI machine learning repository, 2017.
- [16] Siwei Feng and Han Yu. Multi-participant multi-class vertical federated learning. *arXiv preprint arXiv:2001.11154*, 2020.
- [17] Martin Franke, Ziad Sehili, and Erhard Rahm. Primat: a toolbox for fast privacy-preserving matching. *Proceedings of the VLDB Endowment*, 12(12):1826–1829, 2019.
- [18] Ian Goodfellow, Yoshua Bengio, Aaron Courville, and Yoshua Bengio. *Deep learning*, volume 1. MIT press Cambridge, 2016.
- [19] Bin Gu, Zhiyuan Dang, Xiang Li, and Heng Huang. Federated doubly stochastic kernel learning for vertically partitioned data. In *Proceedings of the 26th ACM SIGKDD International Conference on Knowledge Discovery & Data Mining*, pages 2483–2493, 2020.
- [20] Bin Gu, An Xu, Zhouyuan Huo, Cheng Deng, and Heng Huang. Privacy-preserving asynchronous federated learning algorithms for multi-party vertically collaborative learning. *arXiv preprint arXiv:2008.06233*, 2020.
- [21] Stephen Hardy, Wilko Henecka, Hamish Ivey-Law, Richard Nock, Giorgio Patrini, Guillaume Smith, and Brian Thorne. Private federated learning on vertically partitioned data via entity resolution and additively homomorphic encryption. *arXiv preprint arXiv:1711.10677*, 2017.
- [22] Trung Hoang. Video game dataset. <https://www.kaggle.com/jummyegg/rawg-game-dataset>.
- [23] Housing and Development Board. Resale flat prices in Singapore. <https://data.gov.sg/dataset/resale-flat-prices>.

- [24] Yaochen Hu, Peng Liu, Linglong Kong, and Di Niu. Learning privately over distributed features: An admm sharing approach. *arXiv preprint arXiv:1907.07735*, 2019.
- [25] Yaochen Hu, Di Niu, Jianming Yang, and Shengping Zhou. Fdml: A collaborative machine learning framework for distributed features. In *Proceedings of the 25th ACM SIGKDD International Conference on Knowledge Discovery & Data Mining*, pages 2232–2240, 2019.
- [26] Ali Inan, Murat Kantarcioglu, Gabriel Ghinita, and Elisa Bertino. Private record matching using differential privacy. In *Proceedings of the 13th International Conference on Extending Database Technology*, pages 123–134, 2010.
- [27] Yan Kang, Yang Liu, and Tianjian Chen. Fedmvt: Semi-supervised vertical federated learning with multiview training. *arXiv preprint arXiv:2008.10838*, 2020.
- [28] Alexandros Karakasidis, Georgia Koloniari, and Vassilios S Verykios. Scalable blocking for privacy preserving record linkage. In *Proceedings of the 21th ACM SIGKDD International Conference on Knowledge Discovery and Data Mining*, pages 527–536, 2015.
- [29] Alexandros Karakasidis and Vassilios S Verykios. Secure blocking+ secure matching= secure record linkage. *Journal of Computing Science and Engineering*, 5(3):223–235, 2011.
- [30] Dimitrios Karapiperis, Aris Gkoulalas-Divanis, and Vassilios S Verykios. Federal: A framework for distance-aware privacy-preserving record linkage. *IEEE Transactions on Knowledge and Data Engineering*, 30(2):292–304, 2017.
- [31] Dimitrios Karapiperis and Vassilios S Verykios. An lsh-based blocking approach with a homomorphic matching technique for privacy-preserving record linkage. *IEEE Transactions on Knowledge and Data Engineering*, 27(4):909–921, 2014.
- [32] Mehmet Kuzu, Murat Kantarcioglu, Ali Inan, Elisa Bertino, Elizabeth Durham, and Bradley Malin. Efficient privacy-aware record integration. In *Proceedings of the 16th International Conference on Extending Database Technology*, pages 167–178, 2013.
- [33] Qinbin Li, Zeyi Wen, Zhaomin Wu, Sixu Hu, Naibo Wang, Yuan Li, Xu Liu, and Bingsheng He. A survey on federated learning systems: vision, hype and reality for data privacy and protection. *arXiv preprint arXiv:1907.09693*, 2019.
- [34] Yang Liu, Yan Kang, Chaoping Xing, Tianjian Chen, and Qiang Yang. A secure federated transfer learning framework. *IEEE Intelligent Systems*, 35(4):70–82, 2020.
- [35] Yang Liu, Yan Kang, Xinwei Zhang, Liping Li, Yong Cheng, Tianjian Chen, Mingyi Hong, and Qiang Yang. A communication efficient collaborative learning framework for distributed features. *arXiv preprint arXiv:1912.11187*, 2019.
- [36] Yang Liu, Yingting Liu, Zhijie Liu, Yuxuan Liang, Chuishi Meng, Junbo Zhang, and Yu Zheng. Federated forest. *IEEE Transactions on Big Data*, 2020.
- [37] Yang Liu, Xiong Zhang, and Libin Wang. Asymmetrically vertical federated learning. *arXiv preprint arXiv:2004.07427*, 2020.
- [38] Kevin P Murphy. Conjugate bayesian analysis of the gaussian distribution. *def*, 1(2 σ):16, 2007.
- [39] Alexandros Nathan and Diego Klabjan. Optimization for large-scale machine learning with distributed features and observations. In *International Conference on Machine Learning and Data Mining in Pattern Recognition*, pages 132–146. Springer, 2017.
- [40] Richard Nock, Stephen Hardy, Wilko Henecka, Hamish Ivey-Law, Giorgio Patrini, Guillaume Smith, and Brian Thorne. Entity resolution and federated learning get a federated resolution. *arXiv preprint arXiv:1803.04035*, 2018.
- [41] Zhongang Qi, Saeed Khorrarn, and Fuxin Li. Visualizing deep networks by optimizing with integrated gradients. In *CVPR Workshops*, volume 2, 2019.
- [42] Qichen Qiu. Kaggle dataset: housing price in Beijing. <https://www.kaggle.com/ruiqurm/lianjia>.
- [43] Russell Reed and Robert J MarksII. *Neural smithing: supervised learning in feedforward artificial neural networks*. Mit Press, 1999.

- [44] Daniele Romanini, Adam James Hall, Pavlos Papadopoulos, Tom Titcombe, Abbas Ismail, Tudor Cebere, Robert Sandmann, Robin Roehm, and Michael A Hoeh. Pyvertical: A vertical federated learning framework for multi-headed splitnn. *arXiv preprint arXiv:2104.00489*, 2021.
- [45] Rory Sayres, Ankur Taly, Ehsan Rahimy, Katy Blumer, David Coz, Naama Hammel, Jonathan Krause, Arunachalam Narayanaswamy, Zahra Rastegar, Derek Wu, et al. Using a deep learning algorithm and integrated gradients explanation to assist grading for diabetic retinopathy. *Ophthalmology*, 126(4):552–564, 2019.
- [46] Rainer Schnell. Efficient private record linkage of very large datasets. International Statistical Institute, 2013.
- [47] Shreya Sharma, Chaoping Xing, Yang Liu, and Yan Kang. Secure and efficient federated transfer learning. In *2019 IEEE International Conference on Big Data (Big Data)*, pages 2569–2576. IEEE, 2019.
- [48] Rebecca C Steorts, Samuel L Ventura, Mauricio Sadinle, and Stephen E Fienberg. A comparison of blocking methods for record linkage. In *International conference on privacy in statistical databases*, pages 253–268. Springer, 2014.
- [49] Chang Sun, Lianne Ippel, Johan Van Soest, Birgit Wouters, Alexander Malic, Onaopepo Adekunle, Bob van den Berg, Ole Mussmann, Annemarie Koster, Carla van der Kallen, et al. A privacy-preserving infrastructure for analyzing personal health data in a vertically partitioned scenario. In *MedInfo*, pages 373–377, 2019.
- [50] Mukund Sundararajan, Ankur Taly, and Qiqi Yan. Axiomatic attribution for deep networks. In *International Conference on Machine Learning*, pages 3319–3328. PMLR, 2017.
- [51] New York City Taxi and Limousine Commission. TLC trip record data. <https://www1.nyc.gov/site/tlc/about/tlc-trip-record-data.page>.
- [52] Zhihua Tian, Rui Zhang, Xiaoyang Hou, Jian Liu, and Kui Ren. Federboost: Private federated learning for gbdt. *arXiv preprint arXiv:2011.02796*, 2020.
- [53] Onno Valkering and Adam Belloum. Privacy-preserving record linkage with spark. In *2019 19th IEEE/ACM International Symposium on Cluster, Cloud and Grid Computing (CCGRID)*, pages 440–448. IEEE, 2019.
- [54] Dinusha Vatsalan and Peter Christen. Privacy-preserving matching of similar patients. *Journal of biomedical informatics*, 59:285–298, 2016.
- [55] Dinusha Vatsalan, Peter Christen, and Vassilios S Verykios. Efficient two-party private blocking based on sorted nearest neighborhood clustering. In *Proceedings of the 22nd ACM international conference on Information & Knowledge Management*, pages 1949–1958, 2013.
- [56] Dinusha Vatsalan, Ziad Sehili, Peter Christen, and Erhard Rahm. Privacy-preserving record linkage for big data: Current approaches and research challenges. In *Handbook of Big Data Technologies*, pages 851–895. Springer, 2017.
- [57] Praneeth Vepakomma, Otkrist Gupta, Tristan Swedish, and Ramesh Raskar. Split learning for health: Distributed deep learning without sharing raw patient data. *arXiv preprint arXiv:1812.00564*, 2018.
- [58] Praneeth Vepakomma, Abhishek Singh, Otkrist Gupta, and Ramesh Raskar. Nopeek: Information leakage reduction to share activations in distributed deep learning. *arXiv preprint arXiv:2008.09161*, 2020.
- [59] Anushka Vidanage, Thilina Ranbaduge, Peter Christen, and Rainer Schnell. Efficient pattern mining based cryptanalysis for privacy-preserving record linkage. In *2019 IEEE 35th International Conference on Data Engineering (ICDE)*, pages 1698–1701. IEEE, 2019.
- [60] Chang Wang, Jian Liang, Mingkai Huang, Bing Bai, Kun Bai, and Hao Li. Hybrid differentially private federated learning on vertically partitioned data. *arXiv preprint arXiv:2009.02763*, 2020.
- [61] Song WenJie and Shen Xuan. Vertical federated learning based on dfp and bfgs. *arXiv preprint arXiv:2101.09428*, 2021.
- [62] Yuncheng Wu, Shaofeng Cai, Xiaokui Xiao, Gang Chen, and Beng Chin Ooi. Privacy preserving vertical federated learning for tree-based models. *arXiv preprint arXiv:2008.06170*, 2020.
- [63] www.salary.sg. Secondary school rankings in Singapore. <https://www.salary.sg/2020/secondary-schools-ranking-2020-psle-cut-off/>.

- [64] Runhua Xu, Nathalie Baracaldo, Yi Zhou, Ali Anwar, James Joshi, and Heiko Ludwig. Fedv: Privacy-preserving federated learning over vertically partitioned data. *arXiv preprint arXiv:2103.03918*, 2021.
- [65] Kai Yang, Tao Fan, Tianjian Chen, Yuanming Shi, and Qiang Yang. A quasi-newton method based vertical federated learning framework for logistic regression. *arXiv preprint arXiv:1912.00513*, 2019.
- [66] Qiang Yang, Yang Liu, Tianjian Chen, and Yongxin Tong. Federated machine learning: Concept and applications. *ACM Transactions on Intelligent Systems and Technology (TIST)*, 10(2):1–19, 2019.
- [67] Shengwen Yang, Bing Ren, Xuhui Zhou, and Liping Liu. Parallel distributed logistic regression for vertical federated learning without third-party coordinator. *arXiv preprint arXiv:1911.09824*, 2019.
- [68] Yang You, Jing Li, Sashank Reddi, Jonathan Hseu, Sanjiv Kumar, Srinadh Bhojanapalli, Xiaodan Song, James Demmel, Kurt Keutzer, and Cho-Jui Hsieh. Large batch optimization for deep learning: Training bert in 76 minutes. *arXiv preprint arXiv:1904.00962*, 2019.
- [69] Qingsong Zhang, Bin Gu, Cheng Deng, and Heng Huang. Secure bilevel asynchronous vertical federated learning with backward updating. *arXiv preprint arXiv:2103.00958*, 2021.
- [70] Yifei Zhang and Hao Zhu. Additively homomorphical encryption based deep neural network for asymmetrically collaborative machine learning. *arXiv preprint arXiv:2007.06849*, 2020.

A Proof of Theorem 1

Theorem 1. Given a finite set of perturbed similarities s_{ij} ($i \in S$) between $|S|$ bloom-filters b_i^A ($i \in S$) in party A and one bloom filter k_j^B in party B, if an attacker knows the scaling parameters μ_0, σ_0 and follows the procedure of the attack method, the probability of the attacker's predicted bloom filter \hat{k}_j^B equaling the real bloom filter k_j^B is bounded by a constant τ . Formally,

$$\Pr \left[\hat{k}_j^B = k_j^B \mid \{s_{ij} \mid i \in S\}, \{k_i^A \mid i \in S\}, \mu_0, \sigma_0 \right] \leq \tau = \text{erf} \left(\frac{\sqrt{\sigma^2 + 1}}{2\sqrt{2}\sigma\sigma_0} \right)$$

where $\text{erf}(\cdot)$ is error function, i.e., $\text{erf}(x) = \frac{2}{\sqrt{\pi}} \int_0^x e^{-t^2} dt$.

Proof. According to the attack method, the attacker can predict based on any $|S|$ bloom filters in party A and their corresponding distances. We denote the negative distance between k_i^A and k_j^B as $l_{ij} = -\text{dist}(k_i^A, k_j^B)$. The attacker's predicted value of l_{ij} is denoted as \hat{l}_{ij} . Then, we have

$$\begin{aligned} & \Pr \left[\hat{k}_j^B = k_j^B \mid \{s_{ij} \mid i \in S\}, \{k_i^A \mid i \in S\}, \mu_0, \sigma_0 \right] \\ &= \Pr \left[\hat{k}_j^B = k_j^B, \{\hat{l}_{ij} = l_{ij} \mid i \in S\} \mid \{s_{ij} \mid i \in S\}, \{k_i^A \mid i \in S\}, \mu_0, \sigma_0 \right] \\ &= \Pr \left[\hat{k}_j^B = k_j^B \mid \{\hat{l}_{ij} = l_{ij} \mid i \in S\}, \{k_i^A \mid i \in S\}, \mu_0, \sigma_0 \right] \\ & \quad \cdot \Pr \left[\{\hat{l}_{ij} = l_{ij} \mid i \in S\} \mid \{s_{ij} \mid i \in S\}, \{k_i^A \mid i \in S\}, \mu_0, \sigma_0 \right] \\ &= \Pr \left[\hat{k}_j^B = k_j^B \mid \{\hat{l}_{ij} = l_{ij} \mid i \in S\}, \{k_i^A \mid i \in S\}, \mu_0, \sigma_0 \right] \Pr \left[\{\hat{l}_{ij} = l_{ij} \mid i \in S\} \mid \{s_{ij} \mid i \in S\} \right] \\ &= \Pr \left[\hat{k}_j^B = k_j^B \mid \{\hat{l}_{ij} = l_{ij} \mid i \in S\}, \{k_i^A \mid i \in S\}, \mu_0, \sigma_0 \right] \prod_{i \in S} \Pr \left[\hat{l}_{ij} = l_{ij} \mid s_{ij} \right] \end{aligned} \quad (3)$$

The first equation holds because of the assumption that the attacker predicts k_j^B through the most likely distance \hat{l}_{ij} , and correctly predicting the $|S|$ correct distances is the prerequisite of predicting the correct bloom filter k_j^B , i.e., $\{\hat{k}_j^B = k_j^B\} \subseteq \{\hat{l}_{ij} = l_{ij} \mid i \in S\}$. The second equation holds because of the definition of conditional probability. The third equation holds because the attacker predicts distances independently based on perturbed similarities. The fourth equation holds because all the \hat{l}_{ij} ($i \in S$) are predicted independently from the corresponding s_{ij} .

According to the attack method, the attacker first predicts the similarity $\hat{\rho}_{ij}$ based on Maximum a Posteriori (MAP) estimation with one experiment s_{ij} . With Bayes' theorem, we have

$$p(\rho_{ij} \mid s_{ij}) \propto p(s_{ij} \mid \rho_{ij})p(\rho_{ij}) \quad (4)$$

Since $\rho_{ij} \sim N(0, 1)$ and $s_{ij} \sim N(\rho_{ij}, \sigma^2)$,

$$p(\rho_{ij} \mid s_{ij}) \sim N \left(\frac{s_{ij}}{\sigma^2 + 1}, \frac{\sigma^2}{\sigma^2 + 1} \right) \quad (5)$$

Note that the posterior distribution is also a Gaussian distribution. This property of Gaussian distribution is also known as *conjugate distribution* [38]. With Equation 5, ρ_{ij} is estimated by

$$\hat{\rho}_{ij} = \arg \max_{\rho_{ij}} p(\rho_{ij} \mid s_{ij}) = \frac{s_{ij}}{\sigma^2 + 1} \quad (6)$$

Then, $\hat{\rho}_{ij}$ is scaled back to distance \hat{l}_{ij}' with known scaling parameters μ_0, σ_0 , i.e.,

$$\hat{l}_{ij}' = \sigma_0 \hat{\rho}_{ij} + \mu_0 \quad (7)$$

Since the distances between the bloom filters are integers, predicting the correct distance, i.e., $\hat{l}_{ij} = l_{ij}$, implies that

$$\begin{aligned} l_{ij} &= \sigma_0 \rho_{ij} + \mu_0 \\ |\hat{l}_{ij}' - l_{ij}| &\leq \frac{1}{2} \end{aligned} \quad (8)$$

With Equation 6, 7 and 8, we can evaluate $\Pr[\hat{l}_{ij} = l_{ij} \mid s_{ij}]$ by

$$\Pr[\hat{l}_{ij} = l_{ij} \mid s_{ij}] = \Pr \left[|\hat{l}_{ij}' - l_{ij}| \leq \frac{1}{2} \mid s_{ij} \right] = \Pr \left[\left| \rho_{ij} - \frac{s_{ij}}{\sigma^2 + 1} \right| \leq \frac{1}{2\sigma_0} \mid s_{ij} \right] \quad (9)$$

Note that we already know the probability density function $p(\rho_{ij} \mid s_{ij})$ in Equation 5. By shifting the mean of the distribution, we have

$$p \left(\rho_{ij} - \frac{s_{ij}}{\sigma^2 + 1} \mid s_{ij} \right) \sim N \left(0, \frac{\sigma^2}{\sigma^2 + 1} \right) \quad (10)$$

Considering Equation 9 and 10, $\Pr[\hat{l}_{ij} = l_{ij} | s_{ij}]$ can be calculated by a simple integral

$$\Pr[\hat{l}_{ij} = l_{ij} | s_{ij}] = \int_{-\frac{1}{2\sigma_0}}^{\frac{1}{2\sigma_0}} \frac{\sqrt{\sigma^2 + 1}}{\sqrt{2\pi}\sigma} e^{-\frac{x^2}{2\sigma^2}(\sigma^2 + 1)} dx = \operatorname{erf}\left(\frac{\sqrt{\sigma^2 + 1}}{2\sqrt{2}\sigma\sigma_0}\right) \quad (11)$$

From Equation 3, 9, and 11, we have

$$\begin{aligned} & \Pr\left[\hat{k}_j^B = k_j^B \mid \{s_{ij} | i \in S\}, \{k_i^A | i \in S\}, \mu_0, \sigma_0\right] \\ &= \Pr\left[\hat{k}_j^B = k_j^B \mid \{\hat{l}_{ij} = l_{ij} | i \in S\}, \{k_i^A | i \in S\}, \mu_0, \sigma_0\right] \prod_{i \in S} \Pr\left[\hat{l}_{ij} = l_{ij} \mid s_{ij}\right] \\ &\leq \prod_{i \in S} \Pr[\hat{l}_{ij} = l_{ij} | s_{ij}] \\ &= \left[\operatorname{erf}\left(\frac{\sqrt{\sigma^2 + 1}}{2\sqrt{2}\sigma\sigma_0}\right)\right]^{|S|} \end{aligned} \quad (12)$$

According to the property of error function, $0 < \operatorname{erf}(x) < 1$ for any $x > 0$. Thus, for any set S , we have

$$\Pr\left[\hat{k}_j^B = k_j^B \mid \{s_{ij} | i \in S\}, \{k_i^A | i \in S\}, \mu_0, \sigma_0\right] \leq \operatorname{erf}\left(\frac{\sqrt{\sigma^2 + 1}}{2\sqrt{2}\sigma\sigma_0}\right) \quad (13)$$

□

B Additional Background

FEDERAL [30] is a PPRL framework that theoretically guarantees the indistinguishability of bloom filters. Suppose the size of bloom filters is set to N . For strings, it generates q -grams and encodes q -grams to bloom filters of size N by composite cryptographic hash functions. For numeric values, it first generates N random numbers r_i ($i \in [1, N]$) and sets a threshold t . Next, it determines N hash functions $h_i(x)$

$$h_i(x) = \begin{cases} 1, & x \in [r_i - t, r_i + t] \quad (i \in [1, N]) \\ 0, & \text{otherwise} \end{cases}$$

Each numeric value is hashed by all the functions h_i ($i \in [1, N]$) and is converted to a bloom filter of size N . These bloom filters are used to calculate similarities on an honest-but-curious third party. They prove that all the bloom filters have similar numbers of ones if we properly set the size of bloom filters. Formally, denoting ω as the number of ones in a bloom filter, we have $\Pr[\omega \leq (1 - \epsilon)E[\omega]] < \delta$, where $\epsilon < 1$ and $\delta < 1$ are tolerable deviations. Therefore, attackers cannot infer whether the numeric values are large or small given the bloom filters. This method is adopted in our experiment of hamming-based similarities.

C Additional Experimental Settings

Datasets The basic information of data sets is summarized in Table 4. Dataset A contains labels and is held by party A. Dataset B does not contain labels and is held by party B.

In `house` dataset, dataset A contains housing data in Beijing collected from *lianjia* [42], and dataset B contains renting data in Beijing collected from *Airbnb* [1]. Two parties are linked by longitude and latitude and the task is to predict the housing price. In `taxi` dataset, dataset A contains taxi trajectory data in New York from TLC [51], and dataset B contains bike trajectory data in New York from Citi Bike [3]. Two parties are linked by longitude and latitude of source and destination of the trajectory and the task is to predict the time of the trajectory. In `hdb` dataset, dataset A contains HDB resale data in Singapore collected from Housing and Development Board [23], and dataset B contains recent rankings and locations of secondary schools in Singapore collected from salary.sg [63]. Two parties are linked by longitude and latitude and the task is to predict the HDB resale prices. In `game` dataset, dataset A contains game data including the number of owners, and dataset B contains game data from Steam [12]. dataset B is game ratings from RAWG [22]. Two parties are linked by game titles and the task is to classify games as popular ($\#\text{owners} > 20000$) or unpopular ($\#\text{owners} \leq 20000$) based on ratings, prices, etc. In `song` dataset, dataset A contains timbre values of songs extracted from million song dataset [2], and dataset B contains basic information of songs extracted from FMA dataset [13]. Two parties are linked by the title of songs and the task is to predict the years of songs.

These eight datasets have a wide variety in multiple dimensions. 1) **Matching of common features**: Due to the property of common features, some datasets can be exactly matched (e.g., `syn`, `frog`, `boone` without noise),

Table 4: Basic information of datasets

Dataset	Type	Dataset A			Dataset B			Common features		Task
		#samples	#ft.	ref	#samples	#ft.	ref	#dims	type	
sklearn	Syn	60,000	50	[11]	60,000	50	[11]	5	float	bin-cls
frog	Syn	7,195	19	[14]	7,195	19	[14]	16	float	multi-cls
boone	Syn	130,064	40	[15]	130,064	40	[15]	30	float	bin-cls
house	Real	141,050	55	[42]	27,827	25	[1]	2	float	reg
taxi	Real	200,000	964	[51]	100,000	6	[3]	4	float	reg
hdb	Real	92,095	70	[23]	165	10	[63]	2	float	reg
game	Real	26,987	38	[12]	439,999	86	[22]	1	string	bin-cls
song	Real	349,270	91	[2]	63,147	519	[13]	1	string	reg

Note: “#ft.” means number of features; “Syn” means synthetic; “Real” means real-world; “bin-cls” means binary classification; “multi-cls” means multi-class classification; “reg” means regression.

some datasets can partially exactly matched (e.g, `game`, `song`), and some datasets can only be fuzzy matched (e.g., `house`, `taxi`, `hdb`). 2) **Similarity metric:** These datasets cover three commonly used similarity metrics including Euclidean-based similarity, Levenshtein-based similarity, and Hamming-based similarity. 3) **Task:** The selected datasets cover three common tasks including binary classification, multi-class classification, and regression. We will present the results according to different similarity metrics.⁴

Licenses Our codes are based on Python 3.8 and some public modules but do not include existing codes. We will release our codes under Apache V2 license².

The datasets that we collected for VFL and used in our experiments have different licenses as shown in Table 5. All of them can be used for analysis but only some of them can be shared or used commercially.

Table 5: Licenses of datasets

License	Dataset	Analyze	Adapt	Share	Commercial
CC BY 4.0 ^a	[12, 13]	✓	✓	✓	✓
CC BY-NC-SA 4.0 ^b	[42]	✓	✓	✓	✗
CC0 1.0 ^c	[1, 14, 15, 63]	✓	✓	✓	✓
Singapore Open Data License ^d	[23]	✓	✓	✓	✗
NYCBS Data Use Policy ^e	[3]	✓	✓	✓	✓
Licensing Terms of MSD ^f	[2]	✓	✓	✓	✗
All rights reserved	[22, 51]	✓	✗	✗	✗

^a <https://creativecommons.org/licenses/by/4.0/>

^b <https://creativecommons.org/licenses/by-nc-sa/4.0/>

^c <https://creativecommons.org/publicdomain/zero/1.0/>

^d <https://data.gov.sg/open-data-licence>

^e <https://www.citibikenyc.com/data-sharing-policy>

^f <http://millionsongdataset.com/faq/>

Resources We perform training on a machine with eight RTX-3090 GPUs, two Intel Xeon Gold 6226R CPUs, and 377GB memory. The linkage is performed on another machine with two Intel Xeon Gold 6248R CPUs and 377GB memory. Additional 500GB swap space is needed to link some large datasets like `song`.

Training Details The number of neighbors K is chosen from $\{50, 100\}$. The sizes of hidden layers are chosen from $\{100, 200, 400\}$ and remain consistent across VFL algorithms. The learning rate is chosen from $\{3 \times 10^{-4}, 10^{-3}, 3 \times 10^{-3}, 1 \times 10^{-2}\}$ and weight decay is chosen from $\{10^{-5}, 10^{-4}\}$. Since FedSim and AvgSim process K times more samples per batch compared to other algorithms, their batch sizes are $1/K$ times smaller than the others. The batch size of FedSim and AvgSim are chosen from $\{32, 128\}$, while the batch size of other algorithms are set to 4096. The training is stopped at the best performance on validation set.

²<https://www.apache.org/licenses/LICENSE-2.0>

D Training Time of FedSim

FedSim has more parameters compared with other baselines, thus leading to a longer training time. For each dataset, we train each approach on one empty RTX-3090 GPU and report their training time per epoch in Figure 8.

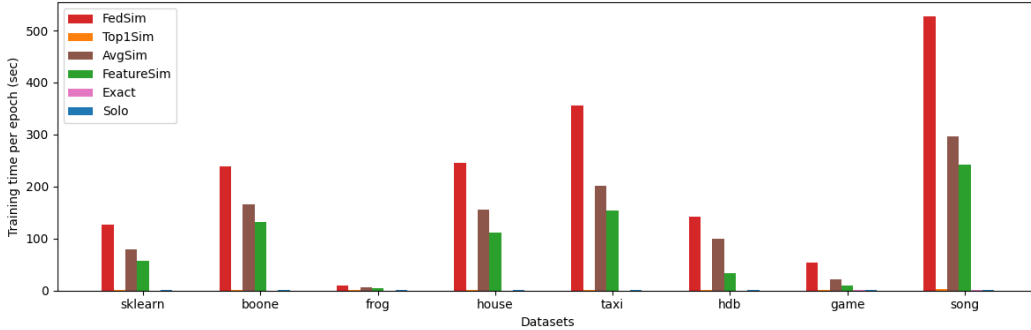


Figure 8: Training time per epoch of different approaches

From Figure 8, we can make two observations. First, FedSim, AvgSim, and FeatureSim requires much more training time than other baselines. This is because these three approaches train K times more samples than other approaches, thus costing K times longer time. Second, FedSim requires about two times longer training time than AvgSim and FeatureSim, which is due to the additional parameters in three gates.

E Choice of K in FedSim

In this subsection, we aim to illustrate that the baselines cannot achieve good performance even by carefully tuning the number of neighbors K . Therefore, with other hyperparameters fixed, we run FedSim and baselines with different K and present their performance in Figure 9.

The trend of each algorithm as K increases well match our expectations. The performance of Top1Sim remains steady since the pairs with largest similarities remain the same. The performance of AvgSim and FeatureSim drops gradually since they cannot handle the increasing data properly, which makes these data bring more noise than information. The performance of FedSim gradually increases and then remains steady, which means FedSim can effectively exploit the information in these additional data. Also, the performance of FedSim may slightly drop when K becomes very large (e.g., $K = 50$ on hdb dataset).

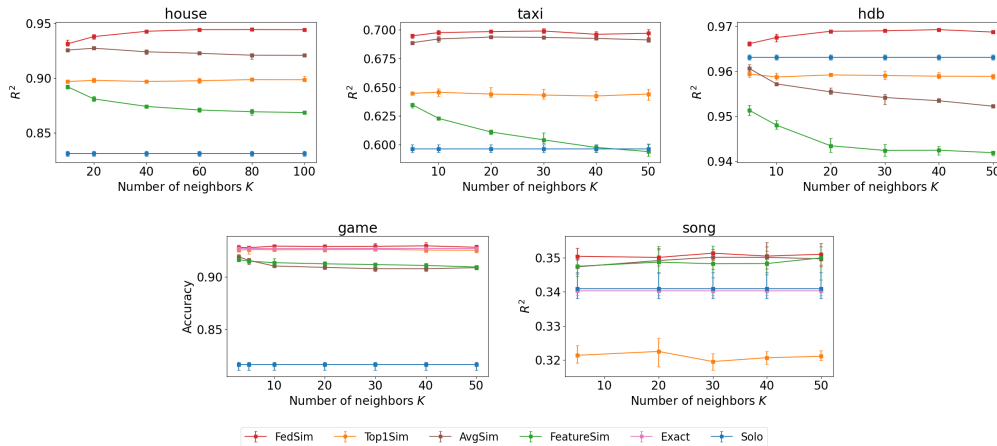


Figure 9: Performance with different K

In conclusion, we can make three observations from Figure 9. First, FedSim consistently outperforms all the baselines under different K . Second, K should be set to a relatively large value to achieve the best performance of FedSim. Third, FedSim can effectively exploit the information from the additional numbers of neighbors while other baselines cannot.

F Discussion

Potential Negative Societal Impact FedSim might be adapted to a linkage attack method, which could threaten the privacy of released data. Since we provide an effective approach to exploit information through fuzzy matched identifiers (e.g. GPS locations), this kind of identifier should be paid special attention to privacy when releasing a dataset.

Consent of Dataset As discussed in Appendix C, all the datasets that we are using are public available for analysis. Therefore, we obtain the consent of using these datasets by following the licenses of these datasets.

Personally Identifiable Information The datasets that we are using do not contain personally identifiable information or offensive contents.

Broader Impact FedSim makes a significant step towards practical VFL by enabling VFL on a wider range of applications that requires fuzzy matching. Although FedSim is designed based on SplitNN, the idea of working directly with similarities can also be developed in other VFL frameworks. We believe this idea can boost the performance of many existing VFL approaches.